The quasi-optical design of the QUaD Telescope

Gary Cahill, Creidhe O'Sullivan, J. Anthony Murphy, William Lanigan, Emily Gleeson, et al.

Gary Cahill, Creidhe O'Sullivan, J. Anthony Murphy, William Lanigan, Emily Gleeson, Peter A. R. Ade, James J. Bock, Melanie Bowden, John E. Carlstrom, Sarah E. Church, Ken Ganga, Walter Gear, John Harris, James Hinderks, Wayne Hu, John Kovac, Andrew Lange, Erik M. Leitch, Bruno Maffei, Olivier Mallie, Simon Melhuish, Angiola Orlando, Giampaolo Pisano, Lucio Piccirillo, Clem Pryke, Ben Rusholme, Andy Taylor, Keith L. Thompson, Michael Zemcov, "The quasi-optical design of the QUaD Telescope," Proc. SPIE 5498, Millimeter and Submillimeter Detectors for Astronomy II, (8 October 2004); doi: 10.1117/12.551680

SPIE.

Event: SPIE Astronomical Telescopes + Instrumentation, 2004, Glasgow, United Kingdom

The Quasi-Optical Design of the QUaD Telescope

Gary Cahill[*a], Créidhe O'Sullivan[a], J. Anthony Murphy[a], William Lanigan[a], Emily Gleeson[a], Peter Ade[b], James Bock[c], Melanie Bowden[b], John Carlstrom[d], Sarah Church[e], Ken Ganga[f], Walter Gear[b], John Harris[b], James Hinderks[e], Wayne Hu[d], John Kovac[d], Andrew Lange[g], Eric Leitch[d], Bruno Maffei[b], Olivier Mallie[b], Simon Melhuish[b], Angiola Orlando[b], Giampaolo Pisano[b], Lucio Piccirillo[b], Clem Pryke[d], Ben Rusholme[e], Andy Taylor[h], Keith L. Thompson[e], Michael Zemcov[b].

[a]Department of Experimental Physics, NUI Maynooth, Co. Kildare, Ireland;
[b]Department of Physics and Astronomy, University of Wales, Cardiff, CF24 3YB, UK;
[c]Jet Propulsion Labratory, 4800 Oak Grove Dr., Pasadena, CA 91109, USA;
[d]Department of Astronomy and Astrophysics, Department of Physics, Enrico Fermi Lab, University of Chicago,5640 South Ellis Avenue, Chicago, IL 60637 USA;
[e]Department of Physics, Stanford University, Stanford, CA 94305, USA;
[f]Infrared Processing and Analysis Center, California Institute of Technology, Pasadena, CA 91125, USA;
[g]Division of Physics, Math and Astronomy, California Institute of Technology, Pasadena, CA 91125, USA;
[h]Institute for Astronomy, University of Edinburgh, Royal Observatory, Blackford Hill, Edinburgh, EH9 3HJ, UK

ABSTRACT

QUaD is a ground-based high-resolution (up to $l \approx 2500$) instrument designed to map the polarisation of the Cosmic Microwave Background and to measure its E-mode and B-mode polarisation power spectra [1]. QUaD comprises a bolometric array receiver (100 and 150 GHz) and re-imaging optics on a 2.6-m Cassegrain telescope [2]. It will operate for two years and begin observations in 2005. CMB polarisation measurements will require not only a significant increase in sensitivity over earlier experiments but also a better understanding and control of systematic effects particularly those that contribute to the polarised signal. To this end we have undertaken a comprehensive quasi-optical analysis of the QUaD telescope. In particular we have modelled the effects of diffraction on beam propagation through the system. The corrugated feeds that couple radiation from the telescope to phase-sensitive bolometers need to have good beam symmetry and low sidelobe levels over the required bandwidth. It is especially important that the feed horns preserve the polarisation orientation of the incoming fields. We have used an accurate mode-matching model to design such feed horns. In this paper we present the diffraction analysis of the QUaD front-end optics as well as the electromagnetic design and testing of the QUaD corrugated feeds.

Keywords: quasi-optics, gaussian beam modes, optical design, feed horn design, cosmic microwave background.

1. INTRODUCTION

The Cosmic Microwave Background (CMB) has proven to be an invaluable tool for cosmologists. Sensitive measurements of the temperature anisotropy in particular have made increasingly accurate estimates of the fundamental cosmological parameters. However, in addition to the temperature anisotropy signal there is also an anisotropy in the linear polarisation of the CMB, introduced by Thomson scattering of the photons at re-ionisation. This was recently detected for the first time by the DASI experiment [3]. The polarisation field is generally parameterised in terms of two

[*]Tel +353-1-7084674, Fax. +353-1-7083313, garrett.a.cahill@may.ie

Millimeter and Submillimeter Detectors for Astronomy II, edited by Jonas Zmuidzinas, Wayne S. Holland, Stafford Withington, Proceedings of SPIE Vol. 5498 (SPIE, Bellingham, WA, 2004) · 0277-786X/04/$15 · doi: 10.1117/12.551680

rotationally invariant fields called E(θ,ϕ) and B(θ,ϕ) [4] for easy comparison with theoretical models. Accurate measurements of this polarisation signal, the aim of many of the latest generation of CMB experiments, will give us even more information about processes in the early Universe.

The QUEST (Q and U Extra-galactic Survey Telescope) and DASI (the Degree Angular Scale Interferometer) telescope (the combination now called QUaD) is a ground-based experiment designed to measure the polarisation of the CMB. It will observe from the South Pole and begin operation in 2005. QUaD will measure both the E-mode power spectrum and the much smaller B-mode power spectrum. It is expected to make an important contribution to B-mode surveys in particular and when combined with the four-year WMAP data will improve constraints on many cosmological parameters by up to a factor of two [1].

Experiments such as QUaD require an in-depth understanding and control of systematic effects, particularly those that could contribute to the polarised signal. In this paper we deal specifically with the telescope front-end optics. We first describe the initial design before discussing the feed horns and aspects of the quasi-optical analysis.

2. INITIAL OPTICAL DESIGN

QUaD comprises a bolometric array receiver on a 2.6-m on-axis Cassegrain telescope[2] designed to minimise systematic effects in the polarisation signal. The 0.47-m secondary is supported by a foam cone, maintaining the overall axial symmetry of the system. The focal plane contains 31 pairs of orthogonal polarisation-sensitive bolometers (PSBs)[5]; 12 of the PSB pairs will operate at 100 GHz, the remaining 19 at 150 GHz. Simultaneous observations in bands centred at two frequencies will allow spectral discrimination between CMB and foreground signals. Each pair of PSBs is fed by a single corrugated horn antenna and differenced to give a measure of the *Q* and *U* Stokes parameters in the coordinate frame of the instrument:

$$\Delta I = Q\cos 2\theta + U\sin 2\theta ,$$

where θ is the angle between the instrument co-ordinate system and the sky co-ordinate system. Common-mode signals, such as fluctuations in unpolarised atmospheric emission, are rejected by this differencing scheme.

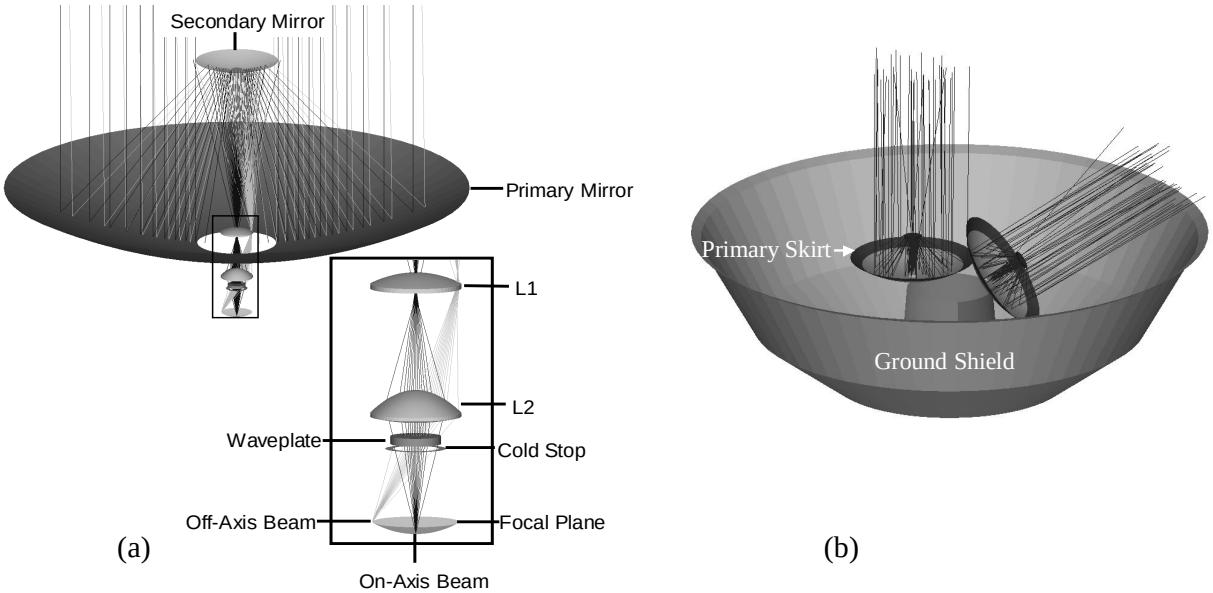

Fig. 1. (a) The QUEST and DASI (QUaD) Telescope front-end optics. (b) The telescope with the ground shield and the skirting around the primary mirror.

The axial symmetry means that instrumental polarisation effects can be measured and removed by rotating the telescope about its axis. In addition there is an achromatic half-waveplate close to the pupil stop of the system (Fig. 1(a)) which can rotate the co-ordinate system of the focal plane with respect to the telescope and sky. As a result each PSB pair can measure both the *Q* and *U* Stoke parameters. Re-imaging optics (two 19-cm diameter lenses) are used to convert the slow beam at the focus of the telescope to an F2.3 focal plane (Fig. 1(a)). This allows a large number of feed horns, giving a high instantaneous sensitivity, and a large (1.5°) field-of-view. The lenses, the waveplate, cold Lyot stop and focal plane are all located inside a 4K cryostat. The primary mirror (imaged at the cold stop) is under-illuminated by the feed horns to minimize ground spillover. This will be further reduced by a 30-cm skirt around the primary mirror where the supporting foam cone for the secondary mirror will be attached. The whole telescope is surround by a ground shield (Fig. 1(b)).

The initial optical design for the telescope was carried out using ray-tracing, a technique which works well at optical wavelengths. As these frequencies, however, the wavelength of the radiation (2mm and 3mm) is an appreciable fraction of the component sizes and diffraction effects become important. We have carried out a quasi-optical analysis to investigate these effects. We analyse the system by first determining the field at the horn apertures and then propagating it through a model of the telescope optics to the sky. In the next section we discuss the beam pattern from the horns.

3. FEED-HORN DESIGN

NUI Maynooth's modelling software (SCATTER[6]), based on a rigorous electromagnetic mode matching technique, was used to develop prototype designs for the QUaD 100- and 150-GHz single-moded corrugated feed horns. These horns have to produce well-controlled beams that satisfy strict criteria with regard to cross-polarisation and sidelobe level. The horns must transmit both orthogonal polarisations. Ordinary corrugated horns, small enough to fit into the cryogenic fridge, do not meet these requirements and so a number of alternative designs (profiled conical and Winston cones) were investigated (see *e.g.* Fig. 2). Suitable feed designs were found for both frequencies and the horns have been manufactured by TK Ltd. (UK). The 100-GHz beam profiles were measured at the NUI Maynooth test range and were found to be in excellent agreement with the theoretical prediction (Fig. 3).

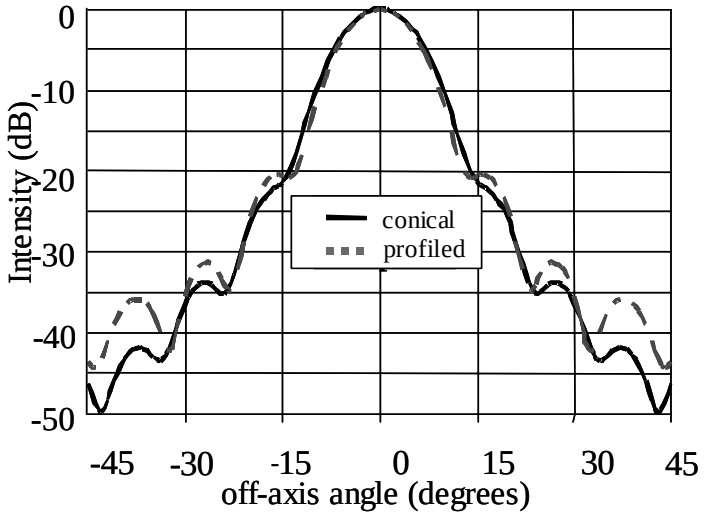

Fig. 2. The narrower far-field beam achieved by profiling a corrugated horn.

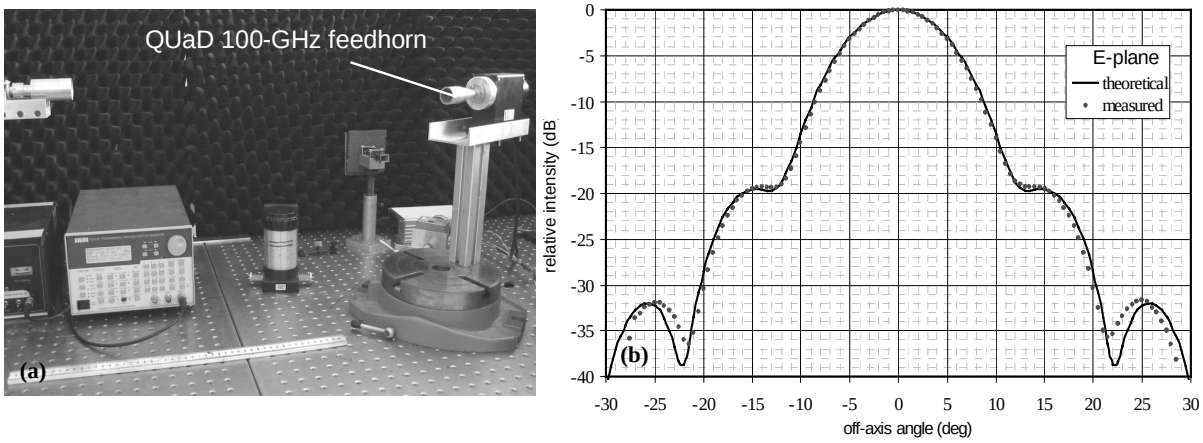

Fig. 3. Measurement of the 100-GHz QUaD horns at NUI Maynooth. (a) QUaD feed horn on the antenna test range and (b) theoretical and measured E-plane beam pattern.

The predicted 100- and 150-GHz QUaD horn beam patterns are shown in Fig. 4. In the QUaD design there is a cold stop in front of the focal plane which will truncate the beams at angles greater than 12.5° (this corresponds to -20dB). Also shown is the best fit Gaussian to each of the beams. Above –20dB these beams are well fit by a Gaussian function. We use the Gaussian approximation for our preliminary quasi-optical analysis.

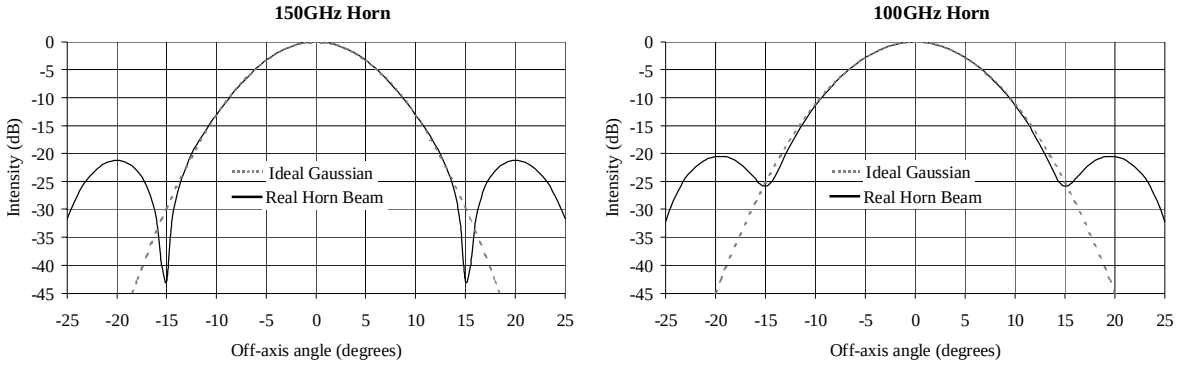

Fig. 4. The predicted QUaD horn beams and the best-fit fundamental Gaussian beam at 100 and 150 GHz.

The upper edge of the frequency bands is defined by filters mounted at the front of each horn antenna. The lower edge is determined by the waveguide connecting each horn to a bolometer cavity at the back. A hybrid mode model[6], where an average surface impedance is assumed for the corrugated guide, was used initially for designing the waveguide filter since there are several corrugations per wavelength. With this approach it is straightforward to predict mode cut-offs in terms of the waveguide radius and slot depths. The mode matching technique was then used to fine-tune the horn-plus-filter design in order to get a smooth band edge at the required frequency. In particular the transition from the deeper corrugations in the filter to the $\lambda/4$ corrugations at the horn mouth had a significant effect on the shape of the band edge[7].

4. QUASI-OPTICAL ANALYSIS

4.1 Method

The quasi-optical analysis was carried out in a number of ways. Gaussian beam mode analysis (GMBA) and the software packages GLAD, Zemax and GRASP8 have all been used to model the telescope. GRASP8 does a full vector physical optics calculation but it cannot model lenses. The other packages use modal techniques to solve the paraxial wave equation. For systems such as QUaD we have found that the approximate techniques agree well with GRASP8 down to –25dB or less[8,9]. These techniques are fast and ideal for the design phase of the telescope. GRASP8 will be used for final verification and accurate cross-polar predictions.

4.2 Phase centre location

The horn antennas should be positioned so that the centre of the beam phase curvature lies on the telescope focal plane. The phase centre position was calculated [10] by first using the mode-matching model to determine the horn aperture field and then propagating this through a quasi-optical model of the telescope. The horn position was varied and the telescope on-axis gain calculated (using an average of several frequencies in each band). The results are shown in Fig. 5. The on-axis gain is a maximum when the phase centre is located on the focal plane. As can be seen the phase centres of the 100- and 150-GHz horns are in different locations with respect to the horn apertures. The difference in horn lengths and phase centre positions results in the front of the 100-GHz horns being 2mm in front of the 150-GHz horns.

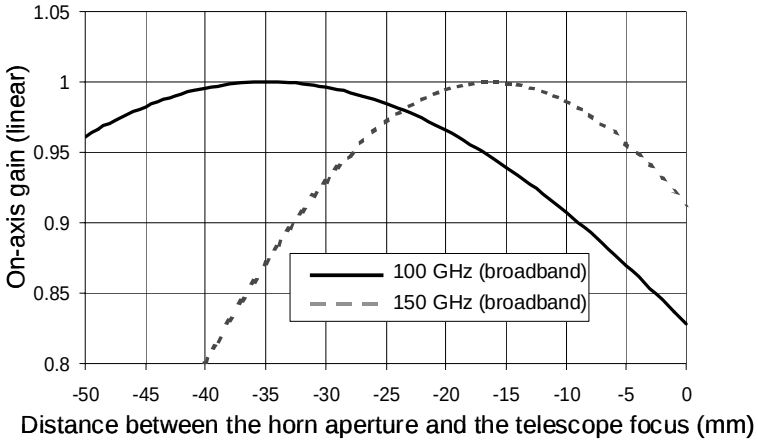

Fig. 5. Plot of on-axis gain as a function of horn position for the 100- and 150-GHz horns. The gain is a maximum when the phase centre is located on the focal plane of the telescope.

Since the beam sidelobe structure is truncated at the cold stop the horns were modelled as Gaussian beams with a radius of 0.6435a at the horn aperture (a is the aperture radius). The phase radius of curvature was taken to be equal to the slant length of the horn.

4.3 Near-field diffraction effects

The effects of diffraction were investigated using GMBA as well as with the commercial software packages GLAD and Zemax (physical optics option). Because of the Cassegrain design, the centre of beams propagating from the feed horn are reflected back from the secondary. These could either be reflected from the front of the cryostat or re-enter the lens system through the cryostat window. In order to reduce the amount of power reflected back into the system, a hole is cut in the centre of the secondary (this hole will also be used to inject a signal of known polarisation directly into the optical system for calibration). The beam reflected back from the secondary should ideally miss the cryostat. However near-field diffraction effects were found to produce some power in the geometrical shadow of the hole (Fig. 6). This 'Poisson spot' effect is not predicted by ray-tracing. In our case the amount of power in the on-axis spike is very small.

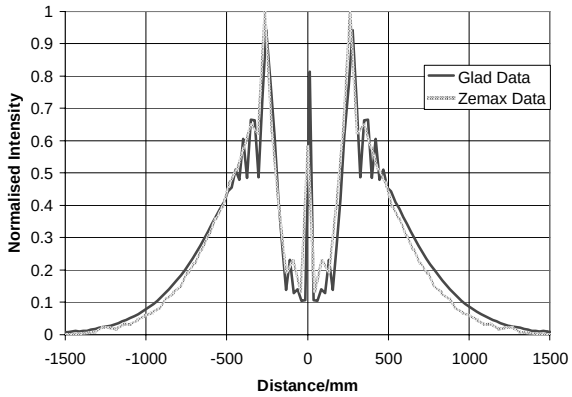

Fig. 6. Zemax POP and GLAD4.7 predictions of the beam pattern at the primary (r=48mm hole, λ = 2.0mm).

4.4 The reflecting collar

For the QuaD design, all the beams do not intersect at the secondary. Off-axis beams are offset from the centre by a small amount. It is therefore not possible to have a sufficiently small hole in the secondary which allows the blocked parts of all beams to terminate on the sky (Fig. 7).

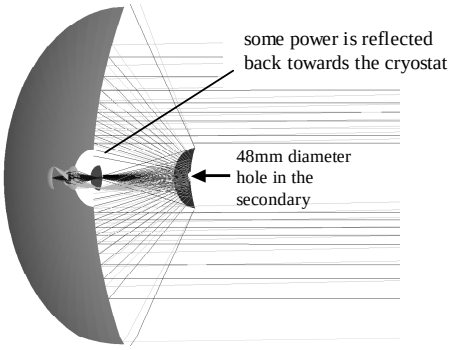

Fig. 7. Ray diagram showing some power being reflected back towards the cryostat from the secondary mirror

It was decided to place a reflecting collar around the cryostat so that this, and any other low-level power that diffracts around the geometrical shadow of the secondary hole (Fig.6), can be reflected back past the secondary and out onto the sky. Ray tracing was used to select a suitable range of designs for the collar and then these were investigated in more detail using a diffraction analysis. The sidelobe patterns predicted by GMBA and the paraxial packages were found to agree closely with those predicted by GRASP8.

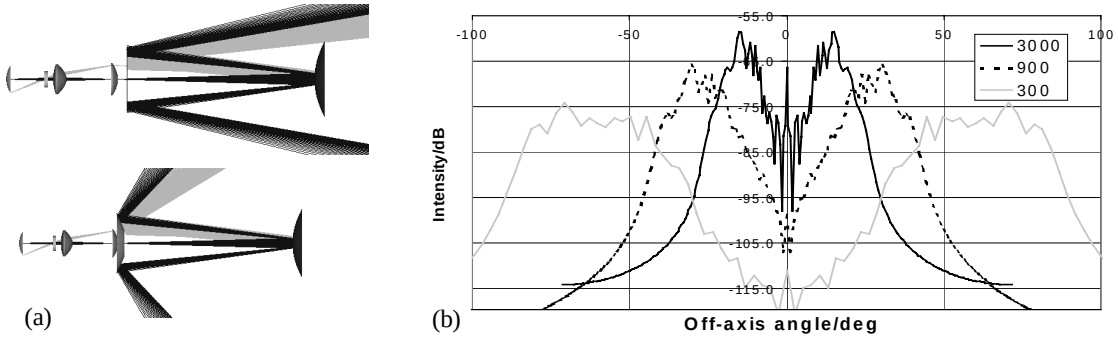

Fig 8 (a) ray-tracing shows the collar designs that will reflect all the power past the secondary mirror. (b) Sidelobe pattern predictions for three parabolic collar designs. The radii of curvature (in mm) are listed in the legend.

4.5 Lens design and coating

Three possible materials were considered for the lenses: silicon (n = 3.4), quartz (n = 2.2) and HDPE (n = 1.58). The different refractive indices, n, mean different curvatures and thicknesses (and therefore transmissions) for the lenses. The manufacturability of the lenses had to be taken into account and highly curved lenses may be difficult to anti-reflection (AR) coat. The waveplate is made from sapphire (n = 3.2).

Perhaps a more important consideration for an experiment such as QUaD is the introduction of instrumental polarisation effects. On propagating out from the focal plane, each beam will travel through six air/material interfaces (due to the waveplate and the two lenses). At each interface there is a difference in transmission for radiation polarised perpendicular or parallel to the plane of incidence (given by the Fresnel coefficients [11]). This difference increases with increasing angle of incidence and will have the effect of producing a small polarisation signal for an unpolarised source (Table 1). It is important that this is minimized.

Angle/Degrees	Average % Transmission	Average % Instrumental Polarization
	150GHz	
0	42.71	0
10.5	41.97	1.17
28	37.08	9.23
	100GHz	
21	38.07	7.52

Table 1: The percentage transmission and instrumental polarisations (difference between parallel and perpendicular polarisations) for a bare (no AR coating) sapphire waveplate and HDPE lenses.

The transmission of the waveplate and lenses can be greatly improved with AR coating. Most coatings have a thickness of $\lambda/4$ and a refractive index of $\sqrt{n_{glass}}$. This ensures that the reflected radiation from the coating interferes destructively with that from the glass. However, QUaD will be observing across two bands: from 81GHz to 102GHz (100GHz band), and from 132GHz to 171GHz (150GHz band). Two options were considered for the thickness of the AR coating; firstly $\lambda/4$ for a wavelength between the centres of the two bands ($\lambda/4$ = 682μm) and secondly a thickness which was close to a multiple of $\lambda/4$ for the centre of both bands (Table 2).

	150GHz/μm	**100GHz/μm**
¼ λ	494.71	819.11
¾ λ	1484.12	**2457.32**
$^5/_4$ λ	**2473.54**	4095.53
$^7/_4$ λ	3462.95	5733.74

Table 2. Matching the two bands so that maximum transmission occurs close to the centres of each band. A thickness of 2465microns was used to model this AR coating.

From Table 2 it can be seen that $^3/_4\lambda$ for the centre of the 100-GHz band is very close to $^5/_4\lambda$ for the centre of the 150-GHz band. An average of these two thicknesses was modelled for each of the lens materials. Fig. 9 shows that the maximum transmission for the 2.465mm coating occurs close to the centre of both the 150-GHz band and the 100-GHz band while the maximum transmission for the 0.682mm coating occurs between both bands. An average transmission for the band was determined by calculating the transmission at the centre frequency and the edges of each band for each horn position on the focal plane (see Fig. 11). The results for the HDPE lenses are listed in Table 3.

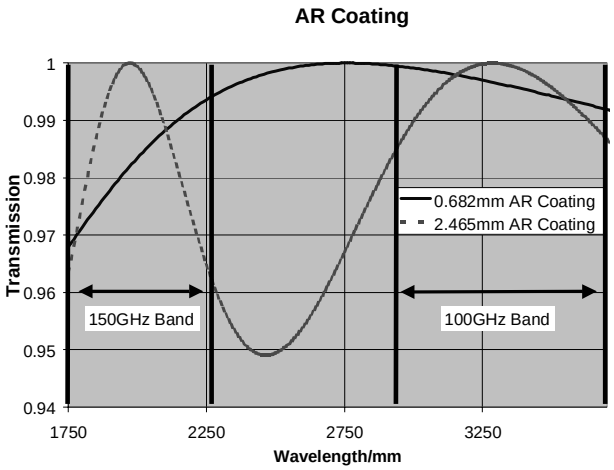

Fig. 9. Transmission as a function of wavelength for an AR coating of thickness 682μm and 2465μm.

	682micron AR coating		2465micron AR coating	
Angle/Degrees	Average % Transmission	Average % Instrumental Polarization	Average % Transmission	Average % Instrumental Polarization
		150GHz		
0	75.5	0	68.5	0
10.5	74.	1.	67.	1.
28	70.	15.	58.	7.
		100GHz		
21	81.	16.	76.	14.

Table 3: Average transmission and instrumental polarisation (difference between transmission for orthogonal polarisations) for the HDPE lens option. (Calculated using the Zemax PO option.) The four different pixel positions (angle to the optic axis) on the focal plane are listed.

With single-layered coatings, the HDPE lenses with a 682-μm thick AR coating give the highest transmission. This is currently the favoured design. Zemax can also be used to estimate the levels of cross-polarisation (Fig. 10), but to accurately calculate such small levels a full physical optics model will be developed.

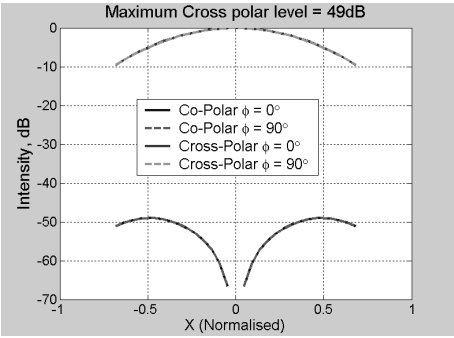

Fig. 10. Estimate of the cross-polarisation for the 150-GHz on-axis pixel.

4.6 Beam pattern predictions

The horn positions on the focal plane are shown in the figure below. Beams were propagated from these positions through a model of the telescope optics using GBMA and the paraxial packages Zemax (PO option) and GLAD. The 150 GHz beam widths and phase radii of curvature at each component are listed in Table 4 (and were similar for all these methods). The values calculated for an on- and off-axis pixel are shown.

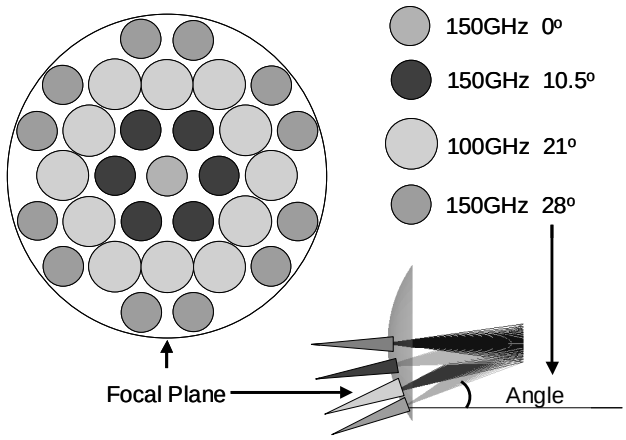

Fig. 11. Horn antenna positions on the focal plane.

	On-Axis Beam				Off-Axis Beam			
Surface	**Beam Size/mm**	**Edge Taper /dB**	**Loss %**	**Phase Radius/mm**	**Beam Size/mm**	**Edge Taper /dB**	**Loss %**	**Phase Radius/mm**
Focal Plane	4.50			Infinity	4.50			Infinity
Cold Stop	25.16	22.39	0.58	180.78	28.74	15.81	2.63	180.78
Waveplate	26.56	30.79	0.08	609.50	30.56	26.86	0.21	782.73
Waveplate	27.27	29.21	0.12	195.41	31.20	28.15	0.15	195.77
L2(surf 1)	31.46	71.09	0.00	522.46	38.22	31.17	0.08	916.78
L2 (surf 2)	35.38	56.20	0.00	-230.44	38.87	18.35	1.46	-231.01
L1 (surf 1)	4.79	3419.14	0.00	-96.10	4.04	136.08	0.00	-309.87
L1 (surf 2)	4.17	4499.76	0.00	343.75	4.29	96.68	0.00	136.23
Filter 1	4.36	6582.19	0.00	95.50	6.02	402.19	0.00	44.88
Filter 2	6.43	3027.59	0.00	55.11	9.52	173.71	0.00	60.47
Secondary Mirror	145.85	23.52	0.44	-195.98	167.05	15.93	2.55	-196.35
Primary Mirror	928.55	19.75	1.06	5028990.00	1055.56	15.22	3.01	-1189310.00
Beam on the Sky	2.44’				3.70’			

Table 4. 150-GHz beam parameters at each of the QUaD optical components. These values were calculated using Zemax (Skew Gaussian Beam). Data are listed for the on- and most off-axis (28°) 150-GHz pixel.

GLAD predictions for the telescope far-field beam patterns of selected pixels are plotted in Fig. 12. These are the main beam predictions, i.e. the beams that are reflected from the primary mirror. There will also be contributions from the beams that pass directly through the hole in the secondary and the beams reflected from the cryostat collar. The relative importance of these components is illustrated in Fig. 13.

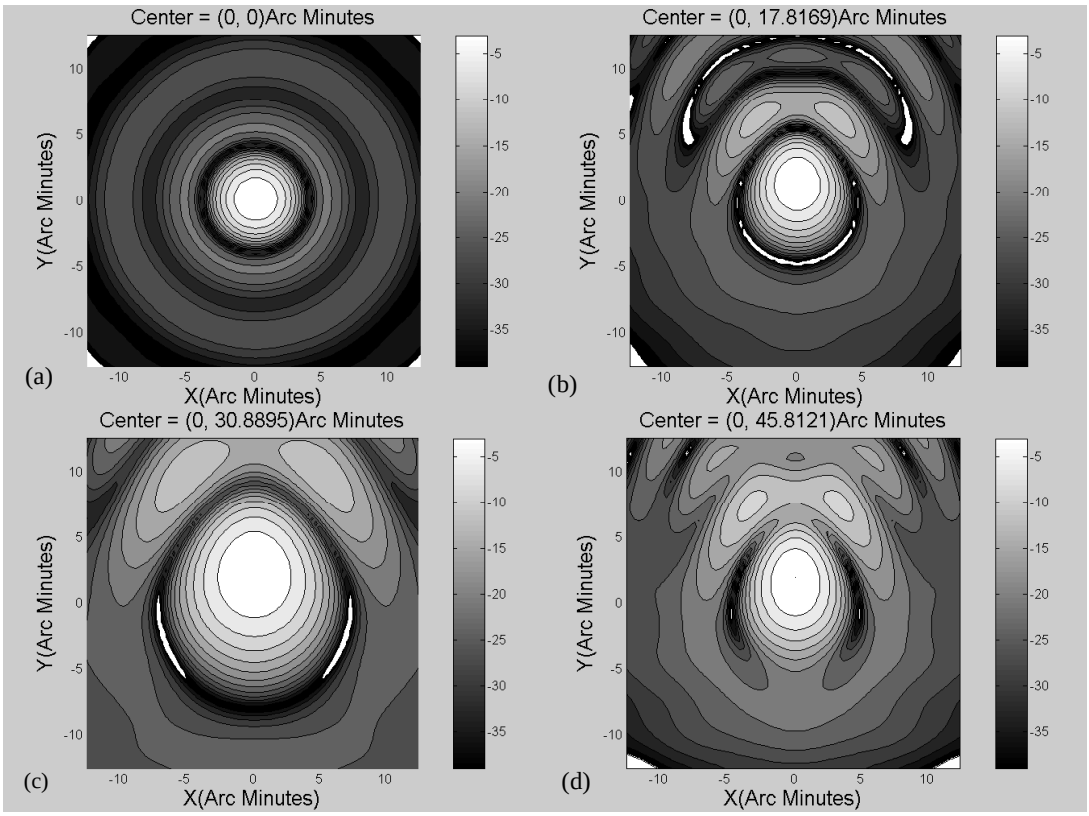

Fig. 12. Far-field beam patterns (predicted by GLAD 4.7 for the (a) on axis 150-GHz horn beam (b) 11^{o} off-axis 150-GHz horn beam (c) 20^{o} off-axis 100GHz horn beam and (d) 28^{o} off-axis 150-GHz horn beam.

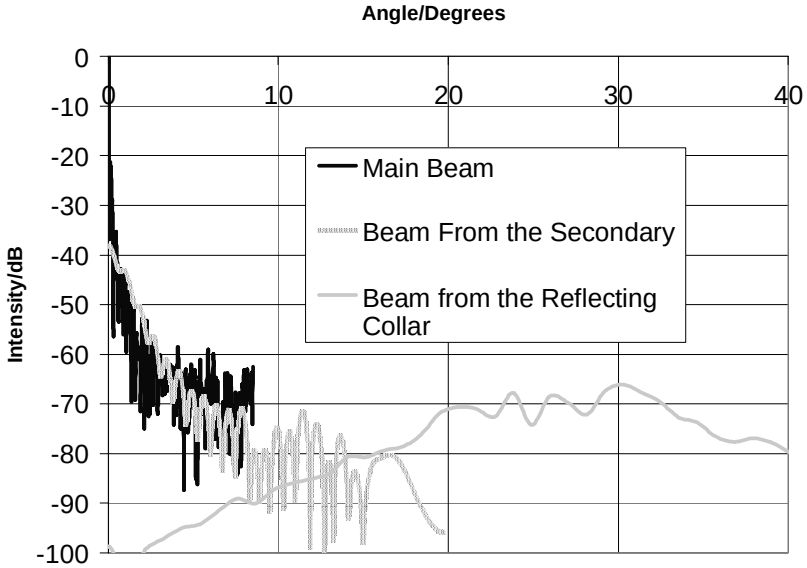

Fig. 13. Beam Pattern on the sky (in dB) as a function of off-axis angle on sky in degrees (100 GHz) showing the main beam (as reflected off the primary), the beam through the hole in the secondary and the beam reflected from an annular conical surface tilted to reflect the radiation through 30 degrees (on-axis pixel).

5. SUMMARY

In this paper we have described the quasi-optical analysis of the QuaD telescope. The initial optical design was developed using a ray-tracing model of the telescope. Ray tracing, although very successful at optical wavelengths, does not take into account the effects of diffraction. In the submillimetre, where the wavelength is an appreciable fraction of component sizes, diffraction is expected to play an important role. We have used a Gaussian beam mode analysis along with the commercial modelling packages, GLAD, Zemax, and GRASP8, to model the telescope optics and include the effect of diffraction.

We have used an electromagnetic mode-matching technique to design the corrugated horn antennas and determine their optimum location on the focal plane. The horn beams were propagated through a quasi-optical model of the telescope and onto the sky in order to determine the beam pattern of each pixel. Quasi-optics were used to determine the best lens coatings and reflecting collar on the cryostat. This diffraction analysis is important for understanding the detailed behaviour of the telescope and minimising any possible systematic effects.

ACKNOWLEDGEMENTS

We would like to thank NUI Maynooth and Enterprise Ireland for supporting this work financially.

REFERENCES

1. M. Bowden et al., "Scientific optimisation of a ground-based CMB polarization experiment", *MNRAS*, **349**, 1, pp. 321-335, 2004.
2. S. Church et al., "QUEST and DASI: a South-Pole CMB polarization experiment" *New Astron. Rev.*, **47** 1083-1089, 2003.
3. J. Kovac, E.M. Leitch, C. Pryke, J.E. Carlstrom, N.W. Halverson, W.L. Holzapfel, "*Detection of polarization in the cosmic microwave background using DASI*", *Nat*, **420**, 772, 2002.
4. M. Zaldarriaga, D.N. Spergel, U. Seljak, "*Microwave Background Constraints on Cosmological Parameters*" *ApJ*, **488**, 1, 1997.
5. W.C. Jones, R. Bhatia, J.J. Bock, A.E. Lange, "A Polarization Sensitive Bolometric Receiver for Observations of the Cosmic Microwave Background" in T.G. Phillips, J. Zmuidzinas, eds., Proc. SPIE, 4855, 227, 2003.
6. J.A. Murphy, R. Colgan, C. O'Sullivan, B. Maffei, P. Ade, "Radiation patterns of multi-moded corrugated horns for far-IR space applications", *Infrared Physics and Technology*, **42**, pp 515-528, 2001.
7. E. Gleeson, W. Lanigan, J. A. Murphy, C. O'Sullivan, B. Maffei, S.E. Church, E. Cartwright, "Bandwidth characteristics of corrugated waveguide-horn feeds for CMB experiments", these proceedings (paper 5498-89).
8. C. O'Sullivan, E. Atad-Ettedgui, W. Duncan, D. Henry, W. Jellema, J.A. Murphy, N. Trappe, H. van de Stadt, S. Withington, G. Yassin, "Far-IR Optics Design and Verification", *Int. Journal IR & Millimeter Waves*, **23**, 7, 2002.
9. G. Yassin, S. Withington, C. O'Sullivan, J.A. Murphy, T. Peacocke, W. Jellema, P. Wesselius, "Electromagnetic simulations of submillimetre-wave systems", Proc. 13th International Symposium on Space Terahertz technology, Harvard, USA, 2002.
10. E. Gleeson *et al*., " 'Phase centres' of Far Infrared Multi-moded Horn Antennas", *Int. J. Infrared & Millimetre Waves*, **23**, 5, 711 – 730, 2002.
11. M. Born, and E. Wolf, "Principles of Optics", Cambridge University Press, 1999.